arXiv:1407.6663v1 [astro-ph.CO] 24 Jul 2014

Planck intermediate results. XXVI. Optical identification and redshifts of *Planck* clusters with the RTT150 telescope

Planck Collaboration: P. A. R. Ade[74], N. Aghanim[51], M. Arnaud[63], M. Ashdown[60,6], J. Aumont[51], C. Baccigalupi[73], A. J. Banday[81,10], R. B. Barreiro[57], R. Barrena[56], N. Bartolo[28], E. Battaner[82,83], K. Benabed[52,80], A. Benoit-Lévy[22,52,80], J.-P. Bernard[81,10], M. Bersanelli[31,45], P. Bielewicz[81,10,73], I. Bikmaev[18,2], H. Böhringer[68], A. Bonaldi[59], L. Bonavera[57], J. R. Bond[9], J. Borrill[13,76], F. R. Bouchet[52,80], R. Burenin[75,70*], C. Burigana[44,29], R. C. Butler[44], E. Calabrese[78], P. Carvalho[6], A. Catalano[64,62], A. Chamballu[63,14,51], H. C. Chiang[25,7], G. Chon[68], P. R. Christensen[72,33], E. Churazov[67,75], D. L. Clements[48], L. P. L. Colombo[21,58], B. Comis[64], F. Couchot[61], A. Curto[6,57], F. Cuttaia[44], H. Dahle[55], L. Danese[73], R. D. Davies[59], R. J. Davis[59], P. de Bernardis[30], A. de Rosa[44], G. de Zotti[41,73], J. Delabrouille[1], J. M. Diego[57], H. Dole[51,50], O. Doré[58,11], M. Douspis[51], A. Ducout[52,48], X. Dupac[36], G. Efstathiou[54], F. Elsner[52,80], T. A. Enßlin[67], H. K. Eriksen[55], F. Finelli[44,46], I. Flores-Cacho[10,81], O. Forni[81,10], M. Frailis[43], E. Franceschi[44], A. Frejsel[72], S. Fromenteau[1,51], S. Galeotta[43], K. Ganga[1], R. T. Génova-Santos[56], M. Giard[81,10], M. Gilfanov[67,75], Y. Giraud-Héraud[1], E. Gjerløw[55], J. González-Nuevo[57,73], K. M. Górski[58,84], A. Gruppuso[44], F. K. Hansen[55], D. Hanson[69,58,9], D. L. Harrison[54,60], A. Hempel[56,34], S. Henrot-Versillé[61], C. Hernández-Monteagudo[12,67], D. Herranz[57], S. R. Hildebrandt[11], E. Hivon[52,80], W. A. Holmes[58], A. Hornstrup[15], W. Hovest[67], K. M. Huffenberger[23], G. Hurier[51], T. R. Jaffe[81,10], W. C. Jones[25], M. Juvela[24], E. Keihänen[24], R. Keskitalo[13], I. Khamitov[79,18], T. S. Kisner[66], R. Kneissl[35,8], J. Knoche[67], M. Kunz[16,51,3], H. Kurki-Suonio[24,40], G. Lagache[51], A. Lasenby[6,60], M. Lattanzi[29], C. R. Lawrence[58], R. Leonardi[36], F. Levrier[62], P. B. Lilje[55], M. Linden-Vørnle[15], M. López-Caniego[57], P. M. Lubin[26], J. F. Macías-Pérez[64], D. Maino[31,45], N. Mandolesi[44,5,29], M. Maris[43], P. G. Martin[9], E. Martínez-González[57], S. Masi[30], S. Matarrese[28], P. Mazzotta[32], J.-B. Melin[14], L. Mendes[36], A. Mennella[31,45], M. Migliaccio[54,60], M.-A. Miville-Deschênes[51,9], A. Moneti[52], L. Montier[81,10], G. Morgante[44], D. Mortlock[48], J. A. Murphy[71], P. Naselsky[72,33], F. Nati[30], P. Natoli[29,4,44], H. U. Nørgaard-Nielsen[15], D. Novikov[48], I. Novikov[72], C. A. Oxborrow[15], L. Pagano[30,47], F. Pajot[51], D. Paoletti[44,46], F. Pasian[43], O. Perdereau[61], L. Perotto[64], F. Perrotta[73], V. Pettorino[39], F. Piacentini[30], M. Piat[1], D. Pietrobon[58], S. Plaszczynski[61], E. Pointecouteau[81,10], G. Polenta[4,42], L. Popa[53], G. W. Pratt[63], S. Prunet[52,80], J.-L. Puget[51], J. P. Rachen[19,67], M. Reinecke[67], M. Remazeilles[59,51,1], C. Renault[64], S. Ricciardi[44], I. Ristorcelli[81,10], G. Rocha[58,11], M. Roman[1], C. Rosset[1], M. Rossetti[31,45], G. Roudier[1,62,58], J. A. Rubiño-Martín[56,34], B. Rusholme[49], M. Sandri[44], D. Scott[20], L. D. Spencer[74], V. Stolyarov[6,60,77], R. Sudiwala[74], R. Sunyaev[67,75], D. Sutton[54,60], A.-S. Suur-Uski[24,40], J.-F. Sygnet[52], J. A. Tauber[37], L. Terenzi[38,44], L. Toffolatti[17,57,44], M. Tomasi[31,45], M. Tristram[61], M. Tucci[16,61], L. Valenziano[44], J. Valiviita[24,40], B. Van Tent[65], L. Vibert[51], P. Vielva[57], F. Villa[44], L. A. Wade[58], B. D. Wandelt[52,80,27], I. K. Wehus[58], D. Yvon[14], A. Zacchei[43], and A. Zonca[26]

(Affiliations can be found after the references)

ABSTRACT

We present the results of approximately three years of observations of *Planck* Sunyaev-Zeldovich (SZ) sources with the Russian-Turkish 1.5-m telescope (RTT150), as a part of the optical follow-up programme undertaken by the *Planck* collaboration. During this time period approximately 20 % of all dark and grey clear time available at the telescope was devoted to observations of *Planck* objects. Some observations of distant clusters were also done at the 6-m Bolshoy Telescope Azimutal'ny (BTA) of the Special Astrophysical Observatory of the Russian Academy of Sciences. In total, deep, direct images of more than one hundred fields were obtained in multiple filters. We identified 47 previously unknown galaxy clusters, 41 of which are included in the *Planck* catalogue of SZ sources. The redshifts of 65 *Planck* clusters were measured spectroscopically and 14 more were measured photometrically. We discuss the details of cluster optical identifications and redshift measurements. We also present new spectroscopic redshifts for 39 *Planck* clusters that were not included in the *Planck* SZ source catalogue and are published here for the first time.

Key words. large-scale structure of Universe – Galaxies: clusters: general – Catalogs

1. Introduction

The *Planck* all-sky survey is the first survey in which a significant number of galaxy clusters have been detected by means of the Sunyaev-Zeldovich (SZ) effect (Sunyaev & Zeldovich 1972) over all the entire extragalactic sky (Planck Collaboration VIII 2011; Planck Collaboration XXIX 2013). Since the SZ signal does not suffer from cosmological dimming and is approximately proportional to cluster mass, the *Planck* SZ galaxy cluster survey contains the most massive clusters in the Universe, and is therefore of unique importance for cluster and cosmological studies.

While blind SZ cluster detection with *Planck* is robust (see, e.g., Planck Collaboration XXIX 2013), further observations of newly detected candidate clusters at other wavelengths are still required. The *Planck* collaboration has undertaken an extensive follow-up programme to confirm *Planck* cluster candidates taken from intermediate versions of the *Planck* SZ catalogue and to measure their redshifts (e.g., Planck Collaboration IX 2011; Planck Collaboration Int. I 2012; Planck Collaboration Int. IV 2013), using the European Northern and Southern observatories (ENO and ESO) and other telescopes. The strategy of this follow-up programme is detailed in Planck Collaboration VIII (2011); Planck Collaboration XXIX (2013).

---

* Corresponding author: R. Burenin rodion@hea.iki.rssi.ru

In this paper, we describe observations with the Russian-Turkish 1.5-m telescope (RTT150[1]). Over three years, approximately 20 % of all clear dark and grey time available at the telescope was used to observe *Planck* SZ sources. Cluster identification procedures are based on those developed for the 400 deg^2 X-ray galaxy cluster survey (400d, Burenin et al. 2007), and for an earlier 160 deg^2 survey (Vikhlinin et al. 1998; Mullis et al. 2003). As was shown with the last two surveys and will be demonstrated below, with 1.5-m class telescopes clusters can be identified at redshifts up to $z \approx 1$, and redshifts can be measured spectroscopically for clusters at approximately $z < 0.4$. Therefore, data taken with such telescopes are sufficient to provide optical identifications and redshift measurements for a large fraction of galaxy clusters detected with *Planck*.

A large fraction of the cluster identifications and redshift measurements presented in this paper were included in the recently published *Planck* SZ source catalogue, (Planck Collaboration XXIX 2013). This companion article presents the details of optical identifications, results of more recent observations at RTT150, and the optical identifications for some *Planck* cluster candidates below the S/N = 4.5 limit of the *Planck* catalogue.

The paper is organised as follows. Section 2 describes the RTT150 telescope and the *Planck* cluster observing programme carried out on it. Sections 3 and 4 review the procedures used for cluster selection and optical identification, and discuss the observations themselves. Finally, Sects. 5 and 6 describe in detail the results of the observations, give examples of cluster identifications, and discuss both individual objects and probable false SZ sources identified in our programme.

2. The RTT150 telescope

The RTT150 optics are of high quality (Aslan et al. 2001) and the telescope site (TÜBİTAK National Observatory, Bakyrlytepe mountain, altitude 2550 m, location $2^h01^m20^s$ E, $36°49'30''$ N) has good astronomical weather. We used the TFOSC instrument (TÜBİTAK Faint Object Spectrograph and Camera), a focal-reducer type spectrograph and camera built at Copenhagen University Observatory. This instrument is similar to ALFOSC at the Nordic Optical Telescope (NOT), also used in the *Planck* follow-up programme of clusters, and to other instruments of this series.

TFOSC is equipped with Bessel, Sloan Digital Sky Survey (SDSS), and other filter-sets. It allows a quick switch between direct imaging and spectroscopic modes, which increases the efficiency of the instrument. The size of the TFOSC field of view in direct-imaging mode is $13'.3 \times 13'.3$, with a $0''.39$ pixel scale. In spectroscopic mode, the instrument allows us to obtain low and medium resolution ($500 \lesssim R \lesssim 5000$) long-slit spectra.

The *Planck* cluster follow-up programme was started at the RTT150 telescope in the summer of 2011. We present here the results of observations obtained through the spring of 2014. During this period approximately 60 *clear* dark and grey nights were used. As previously stated, this corresponds to approximately 20% of total amount of dark and grey clear time available at the telescope. This observing time was provided by the Kazan Federal University (KFU) and the Space Research Institute (IKI), operators of the RTT150 from the Russian side.

Additional observations of clusters at high redshift were made with the 6-m Bolshoy Teleskop Azimutal'nyi (BTA) of the Special Astrophysical Observatory of the Russian Academy of Sciences, using the SCORPIO spectrograph (Moiseev & Afanasyev 2005), which is similar in layout and capabilities to the TFOSC instrument at RTT150 and is optimized for spectroscopic observations of faint objects. We used approximately 32 hours of clear weather at the BTA for the *Planck* cluster follow-up programme.

3. *Planck* cluster selection

The *Planck* catalogue of SZ sources (PSZ1 hereafter, Planck Collaboration XXIX 2013) consists of 1227 sources detected through their SZ effect above S/N=4.5 in the *Planck* frequency maps. The catalogue contains a large fraction of newly confirmed or previously known galaxy clusters but it also contains un-confirmed cluster candidates. The procedures used for cluster selection and identification in the *Planck* cluster survey are discussed in detail in Planck Collaboration XXIX (2013). The main steps are as follows.

Cluster candidates are detected blindly using three different algorithms. The quality of an individual detection is estimated from the significance of the SZ signal, the agreement between the three algorithms, and the frequency spectrum of the cluster candidate.

Cluster candidates are cross-correlated with optical, X-ray, and other SZ catalogues and samples. Detection of X-ray emission from the same hot intracluster gas that *Planck* detects through the SZ effect provides definitive confirmation. Cluster candidates are therefore checked for counterparts in the *ROSAT* All Sky Survey (RASS, Voges et al. 1999, 2000). Since *Planck* detects the most massive and the most X-ray-luminous clusters, *Planck* candidates should be detectable in RASS up to $z \approx 0.3$–0.4. Candidates are also checked for counterparts in the Sloan Digital Sky Survey (SDSS, DR8, Aihara et al. 2011) and the *WISE* all-sky survey (Wright et al. 2010).

Candidates without confirmation from these various steps were sent to observing facilities for follow-up observations to confirm them as clusters and to measure their redshifts. In particular, *Planck* candidates with low-quality images on DSS red plates[2] or without SDSS information, or with low signal-to-noise ratio in RASS, were imaged to the depth needed for finding an optical counterpart and for determination of a photometric redshift. Candidates with galaxy concentrations in SDSS or with high signal-to-noise ratio in RASS were sent for spectroscopic confirmation.

4. Optical identifications and redshift measurements

4.1. Surface number density of galaxies

The most straightforward way to identify galaxy clusters in the optical is through detection of an enhanced surface number density of galaxies. The fields of all cluster candidates were inspected on DSS red plates and then in SDSS images if available. On DSS plates, clusters can be identified at redshifts up to about 0.3, while SDSS images allow reliable identifications at redshifts up to redshift around 0.6. To identify more distant clusters, deeper direct images are necessary. For clusters at $z \approx 0.8$, therefor a 1.5-m class telescope, images in r' and i' with approximately one hour exposures are needed. Clusters at $z \approx 1$ and higher should be observed at larger telescopes. Examples are given in Fig. 1. At lower Galactic latitudes, where the density

---

[1] http://hea.iki.rssi.ru/rtt150/en/

[2] http://stdatu.stsci.edu/dss/

of stars is higher, the galaxy surface density enhancement associated with clusters is easier to detect when stars are excluded[3].

4.2. Red sequence

Spectroscopic redshifts are obtained most effectively from spectra of the brightest galaxies in the central part of the cluster. In order to correctly identify the brightest cluster members, foreground galaxies must be securely rejected. That can be done through detection of a red sequence in the galaxy colour-magnitude relation, formed by early-type cluster member galaxies (Gladders & Yee 2000).

Red galaxies, which form the cluster red sequence, are clearly visible near the centre of clusters, as shown in Fig. 2, where pseudo colour $g'r'i'$ images of a few *Planck* clusters obtained at RTT150 are presented. Figure 3 gives an example of a colour-magnitude diagram of galaxies near the centre of the field of a cluster at $z = 0.227$ (PSZ1 G101.52-29.96, left panel in Fig. 1). One can see that observations of red-sequence galaxies in clusters provide an efficient way to identify clusters and their member galaxies.

Observed red-sequence colours can be used to estimate photometric redshifts. For the purposes of this work, photometric redshifts were calibrated using the data of optical observations obtained earlier during the construction of the 400 deg^2 *ROSAT* PSPC galaxy cluster survey (Burenin et al. 2007). The results of this calibration are shown in Fig. 4. The accuracy of the redshift estimates is $\delta z/(1+z) = 0.027$. These preliminary estimates were used mainly for planning observations. Since the accuracy of photometric redshifts is insufficient for accurate cluster mass function measurements, the redshifts for all confirmed clusters should be measured spectroscopically.

Cluster members identified from a red sequence typically form a well-defined concentration of galaxies, with one brightest cD galaxy in the centre (see, e.g., Fig. 1 and the upper left panel in Fig. 2). In some cases, multiple cD-like galaxies are observed in the centre of a concentration (see, e.g., the right-hand panels in Fig. 2). In some cases, the concentration of cluster galaxies is observed to have two or more peaks, with a few cD-like galaxies at the centre of each peak (see, e.g., the lower left panel in Fig. 2). In our work, the optical centres of galaxy clusters were determined from the positions of cD galaxies found in the centres of these concentrations.

Some galaxy clusters are not associated with prominent enhancements in galaxy surface density. Instead, clusters may be dominated in the optical by one giant central galaxy. These rare objects, called fossil groups (Ponman et al. 1994; Vikhlinin et al. 1999; Jones et al. 2003; Voevodkin et al. 2010), are much less massive than the typical cluster detected by *Planck*. For example, all 12 fossil systems identified in the emph400d survey (Voevodkin et al. 2010) have X-ray luminosities below 10^{44} erg s^{-1}, with corresponding masses below 3×10^{14} M$_\odot$ (see, e.g., Vikhlinin et al. 2009). Nevertheless, objects similar to fossil groups are detected in the *Planck* survey at low redshifts. These objects and their member galaxies can still be reliably identified by their red sequences. An example is discussed in Sect. 6.1.

There are also *Planck* SZ sources where two or more clusters at different redshifts are projected on the sky within a few arcminutes. In those cases, it is not easy to determine the contribution of each cluster to the SZ signal detected by *Planck*.

These, and some other special cases, are discussed in detail below (Sect. 6.2, 6.3).

4.3. Spectroscopic redshift measurements

Once cluster members are identified through a red sequence, the redshift of the cluster as a whole can be determined from the brightest galaxies near the centre of the cluster. For regular clusters, we measured the redshift of the dominant cD galaxy. For less regular clusters, we measured redshifts of 3–5 brightest galaxies, selected using the cluster red sequence observations.

High signal-to-noise ratio is not necessary for accurate spectroscopic redshift determination. Even if individual spectral lines are not well-identified, the redshift can be determined accurately by cross-correlation with an elliptical galaxy template spectrum. Figure 5, for example, shows the spectrum of the brightest central galaxy in a cluster at $z = 0.278$ obtained with the TFOSC spectrometer, along with χ^2 as a function of z from the cross-correlation with an elliptical galaxy template spectrum.

5. Observations

Deep multi-colour observations were obtained for all cluster candidates except those unambiguously detected in SDSS. Images were obtained with the RTT150 telescope and the TFOSC instrument through Sloan $g'r'i'$ filters, typically with 1800 s exposures per filter. Longer exposures were used for cluster candidates with brightest galaxies fainter than $m_{r'} \approx 21$, i.e., which may be located at redshifts $z > 0.7$ (e.g., Vikhlinin et al. 1998). Images were obtained in a series of 300 or 600 s exposures with $\approx 10''$–$30''$ pointing offsets between exposures. Standard CCD calibrations were applied using Iraf[4] software. Individual images in each filter were then aligned and combined. With these data, galaxy clusters can be efficiently identified at redshifts up to $z \approx 1$.

We identified cluster members from a red sequence. Clusters whose photometry indicated $z < 0.4$ were observed spectroscopically with the RTT150. In some cases, clusters whose photometry indicated redshifts above 0.4 were observed spectroscopically with the BTA 6-m telescope and the SCORPIO spectrometer (Sect. 2).

6. Results

The list of *Planck* clusters from the PSZ1 catalogue observed with the RTT150 is given in Table 1. Clusters identified with the RTT150 that were below the PSZ1 signal-to-noise detection limit of $4.5\,\sigma$, and thus not included in the PSZ1 catalogue, are given in Table 2. Coordinates are given of the cluster optical centres, calculated from the position of cD galaxies. The distribution of cluster optical centre offsets from the SZ positions measured with *Planck* is shown in Fig. 6, and is consistent with a two-dimensional Gaussian distribution of width $2'$, in agreement with the *Planck* positional accuracy given in (Planck Collaboration XXIX 2013).

In total, deep direct images of more than one hundred fields in multiple filters were obtained. Forty-seven clusters newly identified using the RTT150 imaging data are marked in Tables 1 (41) and 2 (6). Redshifts of 65 *Planck* clusters were measures spectroscopically, including 12 at high redshift measured with the 6-m BTA telescope. Two of these redshifts were published

---

[3] In our work star–galaxy separation in optical images was performed using SExtractor (Bertin & Arnouts 1996)
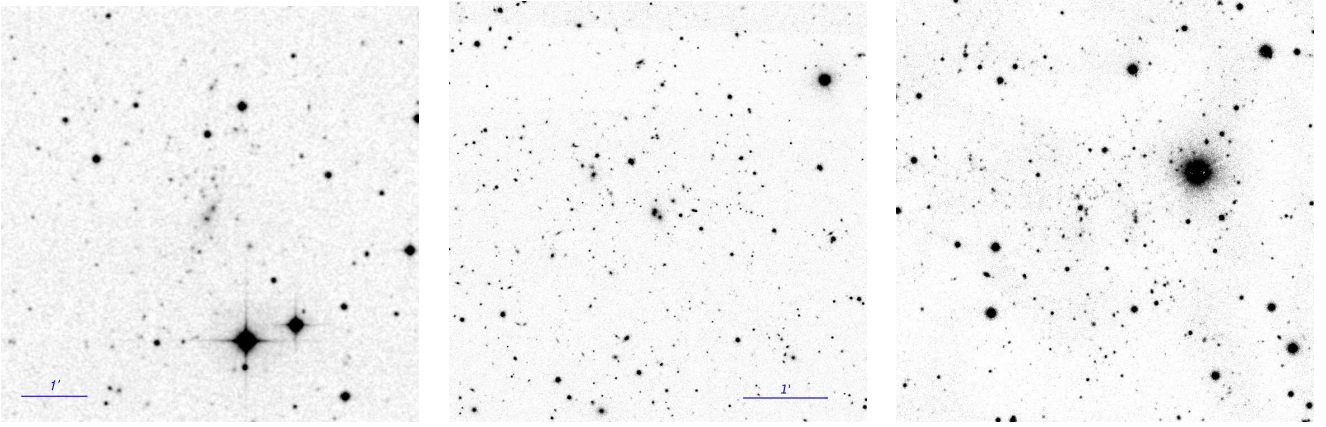
[4] http://iraf.noao.edu/

Fig. 1. Examples of *Planck* galaxy clusters. *Left*: DSS red image of PSZ1 G101.52-29.96 at $z = 0.227$. *Centre*: SDSS i'-band image of PSZ1 G054.94-33.37 at $z = 0.392$. *Right*: deeper RTT150 i'-band image of PSZ1 G108.26+48.66 at $z = 0.674$. The images are approximately 1.5 Mpc on a side at the redshift of the cluster.

Fig. 2. Pseudo colour ($g'r'i'$) RTT150 images of *Planck* clusters, with the colour map adjusted to emphasize the red sequence of galaxies in the centres of clusters. *Upper left*: PSZ1 G098.24-41.15, $z = 0.436$. *Upper right*: PSZ1 G100.18-29.68, $z = 0.485$. *Lower left*: PSZ1 G138.11+42.03, $z = 0.496$. *Lower right*: PSZ1 G209.80+10.23, $z = 0.677$.
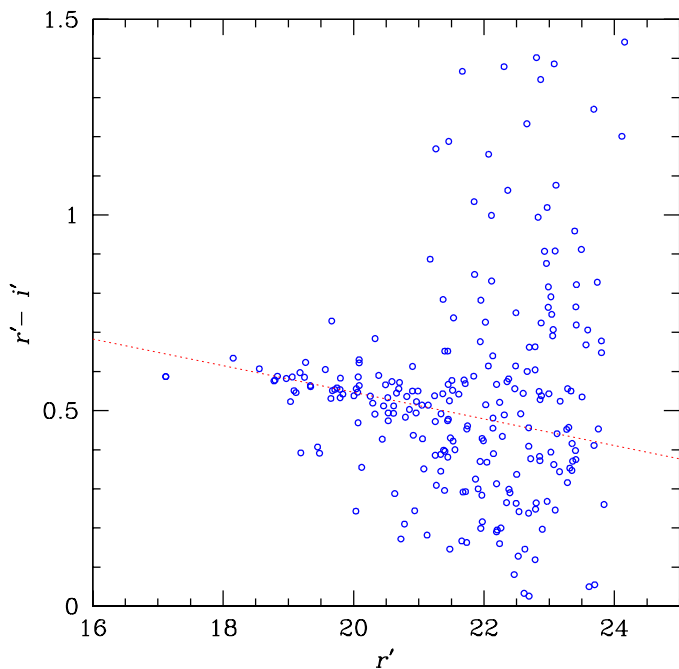
Fig. 3. Colour-magnitude diagram of galaxies near the centre of cluster PSZ1 G101.52-29.96 at $z = 0.227$ (see the left panel in Fig. 1). The best fit red sequence is shown with a dotted line.
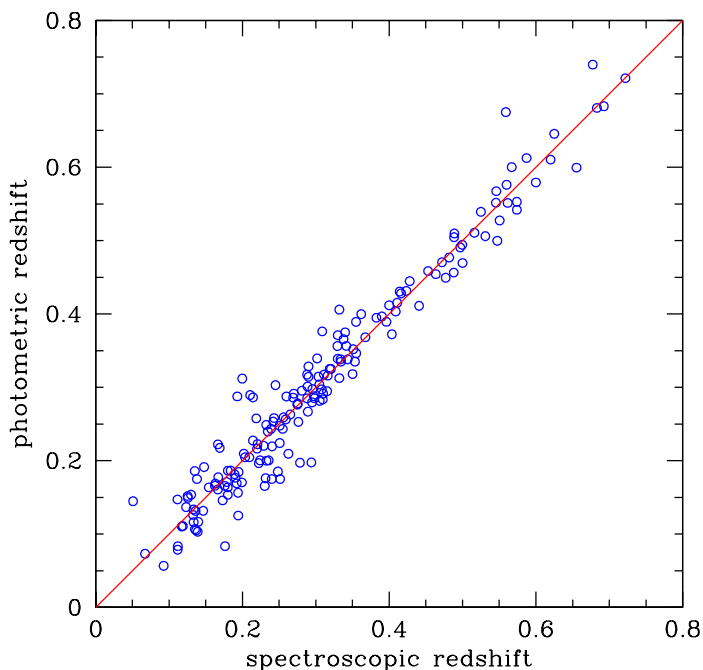

Fig. 4. Comparison of photometric redshifts based on red-sequence colours with spectroscopic redshifts. The points show the data for clusters from the 400d cluster survey (Burenin et al. 2007), which were used for photometric redshift calibration.

in Planck, AMI Collaborations (2013), and 26 were included in the PSZ1 catalogue (Planck Collaboration XXIX 2013).

Table 1 also gives new spectroscopic redshifts measured at the RTT150 for clusters in the PSZ1 catalogue with previously published photometric redshifts (e.g., Wen, Han & Liu 2012), and new photometric redshifts estimated from the RTT150 data of 14 clusters still lacking spectroscopic redshifts.

Below, we give examples of the *Planck* SZ cluster identifications with RTT150 data, showing cases where a 1.5-m-class telescope can be used to identify clusters, while DSS and SDSS data are insufficient for these purposes. We then give notes on some individual objects from Table 1, discuss complicated cases where more data in SZ or X-rays are needed, and identify some probable false clusters among the objects observed in our programme.

6.1. Cluster identification examples

PSZ1 G060.12+11.42: Example of a cluster at low Galactic latitude ($b \approx -11.4°$). From Fig. 7, one can see that it is difficult to identify the surface density enhancement of cluster member galaxies here due to the large number of Galactic stars in the field (left panel, i'-band RTT150 image). This cluster can be identified using the red sequence in the colour-magnitude diagram (right panel). It cannot be identified in DSS, and there are no SDSS imaging data in this field. Additional imaging data were needed, easily obtained with a 1.5-m class telescope.

PSZ1 G076.44+23.53: Example of a cluster with a brightest cluster galaxy much more luminous than other cluster galaxies. Clusters of this type are usually classified as fossil groups (e.g., Voevodkin et al. 2010), see Fig. 8. This cluster appears as almost a single elliptical galaxy in DSS and most of cluster member galaxies are not detected, since they are much fainter than the brightest galaxy. Such clusters are therefore difficult to identify with DSS even at low redshifts, e.g., at $z = 0.169$ in this case. There are no SDSS data in this field. Additional imaging data were thus needed to identify this cluster.

PSZ1 G048.22-65.03: This cluster is too distant to be identified with DSS ($z \approx 0.42$, see Fig. 9). It could have been identified at the depth of SDSS, but there are no SDSS data for this field.

PSZ1 G084.04+58.75: This cluster is too distant to be identified with SDSS ($z = 0.731$, see Fig. 10).

6.2. Notes on individual objects

PSZ1 G066.01-23.30: There is a clear concentration of galaxies that form a well-defined red sequence, shown within the circle in Fig. 11. However, the offset from the SZ source centroid is large, about $4'$, so that there may be astrophysical contamination or some other sources of SZ signal present as well. The spectrum of the central elliptical galaxy in this concentration contains prominent emission lines. From the measured intensity ratio $\lg([NII]\lambda 6583/H\alpha) \approx 0$, we conclude that this galaxy contains a narrow-line AGN (Veilleux & Osterbrock 1987).

PSZ1 G070.91+49.26: In addition to a double cluster at $z = 0.607$, there is also a smaller foreground cluster at $z = 0.458$ (the redshift was also measured at RTT), which should produce an SZ signal. The positions of these clusters in the field centred on the *Planck* SZ source coordinates are shown in Fig. 12. In the published PSZ1 catalogue this SZ source was incorrectly identified with smaller cluster at $z = 0.458$, which should provide only a weak contribution to the measured SZ signal as compared to the more distant and rich double cluster at $z = 0.607$.

Table 1. Clusters from the PSZ1 catalogue observed with the RTT150.

Name	Position (J2000)		z	New ID	Notes
	R. A.	Decl.			
PSZ1 G034.78+31.71	16 58 38.6	+15 19 13	0.480		
PSZ1 G037.69−46.90	21 50 36.8	−16 22 29	0.263	+	
PSZ1 G038.71+24.47	17 31 59.1	+15 40 42	0.0836		
PSZ1 G042.33+17.46	18 04 16.1	+16 02 16	0.50 [a]	+	
PSZ1 G045.54+16.26	18 14 13.3	+18 17 04	0.24 [a]	+	
PSZ1 G046.13+30.75	17 17 05.7	+24 04 18	0.569[c,d]	+	
PSZ1 G048.22−65.03	23 09 51.0	−18 19 57	0.42 [a]	+	
PSZ1 G049.04+25.26	17 43 30.4	+24 44 19	0.141[c]		ACO 2279
PSZ1 G050.07−27.29	20 58 53.0	+01 24 11	0.334[c]		
PSZ1 G054.94−33.37	21 28 23.4	+01 35 37	0.392		
PSZ1 G055.72+17.58	18 25 30.0	+27 44 27	0.194		
PSZ1 G056.76−11.60	20 18 48.2	+15 07 25	0.122[b]		ZwCl 2016.6+1457
PSZ1 G059.20+32.92	17 20 49.9	+35 20 50	0.383[c]	+	
PSZ1 G059.98−18.66	20 50 27.1	+13 45 18	0.221		
PSZ1 G060.12+11.42	18 58 46.0	+29 15 34	0.30 [a]	+	
PSZ1 G063.92−16.75	20 52 51.7	+17 54 23	0.393[b]	+	
PSZ1 G065.13+57.53	15 16 02.0	+39 44 26	0.685[b,d]	+	
PSZ1 G066.01−23.30	21 19 26.2	+15 21 06	0.248[b]	+	
PSZ1 G066.24+20.82	18 27 26.5	+38 14 50	0.278		
PSZ1 G066.41+27.03	17 56 52.6	+40 08 07	0.576[c]		
PSZ1 G067.02−20.80	21 14 01.4	+17 43 14	0.334	+	
PSZ1 G069.92−18.89	21 15 09.6	+21 01 10	0.308	+	
PSZ1 G070.91+49.26	15 56 25.6	+44 40 42	0.607[b,d]		
PSZ1 G071.57−37.96	22 17 15.8	+09 03 10	0.25 [a]		ACO 2429
PSZ1 G073.22+67.57	14 20 40.3	+39 55 11	0.609[c,d]	+	
PSZ1 G076.44+23.53	18 28 21.8	+48 04 29	0.169	+	
PSZ1 G079.33+28.33	18 02 09.6	+51 37 11	0.204		ZwCl 1801.2+5136
PSZ1 G079.88+14.97	19 23 12.1	+48 16 14	0.0998[b]	+	
PSZ1 G080.11−77.29	00 15 24.4	−17 30 34	0.43 [a]	+	
PSZ1 G084.04+58.75	14 49 00.2	+48 33 28	0.731[b,d]	+	
PSZ1 G084.41−12.43	21 37 46.6	+35 35 51	0.273[b]	+	
PSZ1 G085.71+10.67	20 03 13.4	+51 20 51	0.0805[b]	+	
PSZ1 G087.47+37.65	16 57 20.7	+58 28 54	0.113		
PSZ1 G090.82+44.13	16 03 35.1	+59 11 41	0.269[c]		
PSZ1 G092.27−55.73	23 44 23.1	+03 04 42	0.349[c]		
PSZ1 G095.37+14.42	20 14 29.2	+61 23 30	0.119	+	
PSZ1 G098.24−41.15	23 34 24.1	+17 59 23	0.436		
PSZ1 G100.18−29.68	23 21 02.9	+29 12 52	0.485		
PSZ1 G101.52−29.96	23 26 26.6	+29 21 44	0.227		
PSZ1 G102.00+30.69	17 47 13.0	+71 23 17	0.214[b]		ZwCl 1748.0+7125
PSZ1 G106.15+25.76	18 56 51.7	+74 55 53	0.588[b,d]	+	
PSZ1 G107.66−58.31	00 19 37.6	+03 37 49	0.267[c]		
PSZ1 G108.18−11.53	23 22 29.7	+48 46 30	0.336[b,d]		
PSZ1 G108.26+48.66	14 27 04.6	+65 39 47	0.674[b,d]	+	
PSZ1 G109.14−28.02	23 53 12.7	+33 16 11	0.457[c,d]	+	
PSZ1 G114.81−11.80	00 01 14.7	+50 16 33	0.228[b]	+	
PSZ1 G115.70+17.51	22 26 28.3	+78 16 58	0.50 [a]		
PSZ1 G118.40+42.23	13 42 02.2	+74 25 21	0.478	+	
PSZ1 G121.09+57.02	12 59 33.0	+60 04 12	0.344		
PSZ1 G123.55−10.34	00 55 24.4	+52 29 20	0.107[b]	+	
PSZ1 G127.02+26.21	05 58 02.3	+86 13 50	0.574[b,d]	+	
PSZ1 G129.07−24.12	01 20 00.0	+38 25 18	0.425[b]	+	
PSZ1 G130.26−26.53	01 23 39.6	+35 53 58	0.216		ZwCl 0120.8+3538
PSZ1 G134.31−06.57	02 10 25.1	+54 34 09	0.44 [a]	+	
PSZ1 G134.64−11.77	02 02 37.8	+49 26 28	0.207[b]		
PSZ1 G138.11+42.03	10 28 09.7	+70 34 26	0.496	+	
PSZ1 G139.61+24.20	06 21 48.9	+74 42 06	0.267		
PSZ1 G141.73+14.22	04 41 05.8	+68 13 16	0.833[b,d]	+	
PSZ1 G149.38−36.86	02 21 33.8	+21 21 58	0.170		ACO 344

[a] Estimated from RTT photometric data.
[b] Not published in the PSZ1 (Planck Collaboration XXIX 2013)
[c] Spectroscopic redshift. The redshift given in the PSZ1 catalogue (Planck Collaboration XXIX 2013) is photometric.
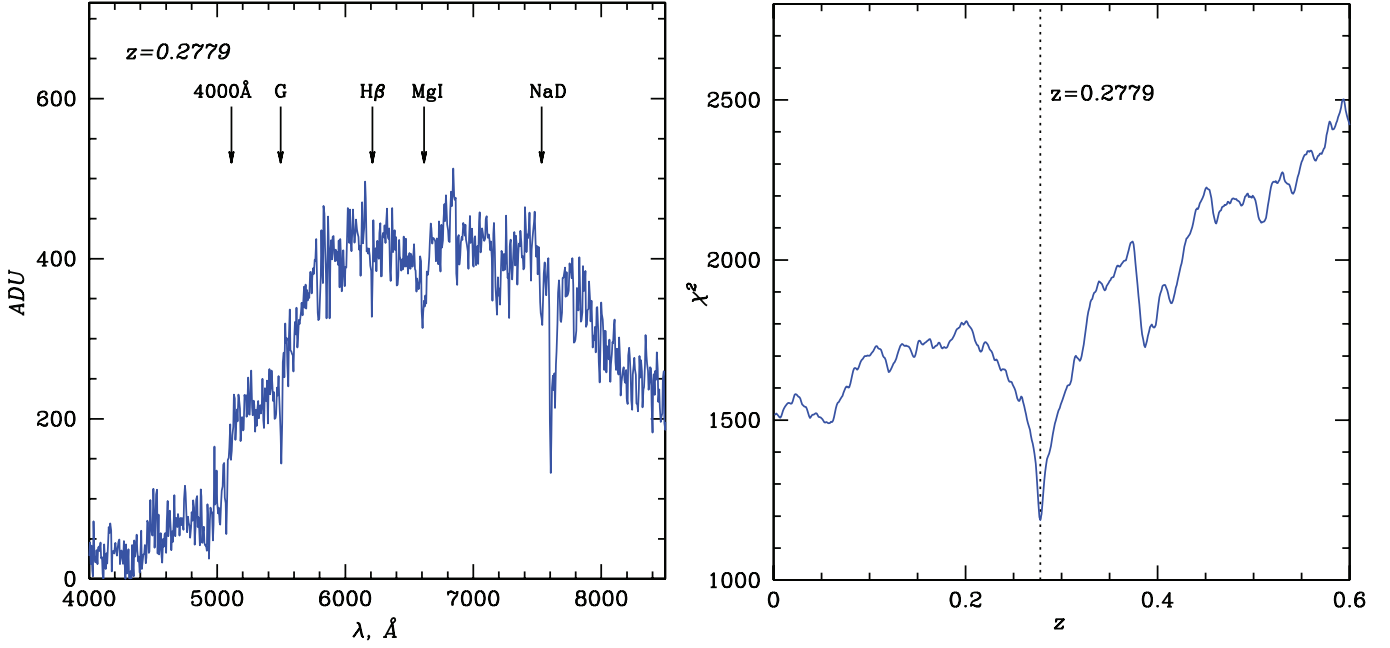[d] Measured at the BTA 6-m telescope of SAO RAS.

Fig. 5. Example of the spectrum of the central elliptical galaxy of cluster at $z = 0.278$ (PSZ1 G066.24+20.82), obtained at RTT150 using the TFOSC spectrometer (left), together with χ^2 from the cross-correlation with an elliptical galaxy template spectrum (right).

Table 1 — continued

Name	Position (J2000) R. A.	Decl.	z	New ID	Notes
PSZ1 G151.80−48.06	02 08 06.5	+10 27 19	0.202[b]		ACO 307
PSZ1 G155.95−72.13	01 30 42.1	−11 51 39	0.620[e]	+	
PSZ1 G156.88+13.48	05 45 41.3	+55 30 40	0.235[b]		
PSZ1 G157.44+30.34	07 48 54.3	+59 42 06	0.45 [a]		[ATZ98] B100
PSZ1 G157.84+21.23	06 40 32.7	+57 45 36	0.43 [a]	+	
PSZ1 G170.22+09.74	06 03 16.8	+42 14 42	0.228[b]		1RXS J060313.4+42123
PSZ1 G171.01+15.93	06 35 47.9	+44 10 15	0.281[b]	+	
PSZ1 G172.93+21.31	07 07 38.1	+44 19 55	0.331	+	
PSZ1 G183.26+12.25	06 43 09.9	+31 50 55	0.85 [a]	+	
PSZ1 G188.56−68.86	02 11 44.2	−17 00 46	0.174[b]		ACO 2985
PSZ1 G205.56−55.75	03 15 22.0	−18 12 22	0.31 [a]	+	
PSZ1 G209.80+10.23	07 22 23.8	+07 24 31	0.677	+	
PSZ1 G216.77+09.25	07 31 20.3	+00 49 24	0.273[c]	+	
PSZ1 G222.75+12.81	07 54 58.6	−02 41 29	0.369	+	
PSZ1 G223.04−20.27	05 54 37.3	−17 44 35	0.19 [a]		ACO 551
PSZ1 G224.01−11.14	06 30 55.3	−14 51 00	0.62 [a]		
PSZ1 G338.97+35.62	14 52 42.2	−18 35 05	0.297[b]	+	

[a] Estimated from RTT photometric data.
[b] Not published in the PSZ1 (Planck Collaboration XXIX 2013)
[c] Spectroscopic redshift. The redshift given in the PSZ1 catalogue (Planck Collaboration XXIX 2013) is photometric.
[d] Measured at the BTA 6-m telescope of SAO RAS.
[e] Redshift from the PSZ1 catalogue, given here for completeness.

PSZ1 G092.27-55.73: While this object was photometrically identified as a double cluster, redshift measurements show that the two cD galaxies separated by $3.'4$ (Fig. 13) are located at significantly different redshifts, $z = 0.3487$ and $z = 0.3387$. The redshift difference is probably too large for a single gravitationally bound object, therefore, this SZ detection likely consists of two projected clusters. It is impossible to separate the members of these two clusters in a photometric red sequence due to their close redshifts. To estimate the richness of each cluster, additional X-ray observations are required or, even better, spectroscopic measurements.

PSZ1 G100.18-29.68: In addition to a rich galaxy cluster at $z = 0.485$, there are also a few foreground elliptical galaxies at $z = 0.178$, indicated with the arrows in Fig. 14. These galaxies can also be identified in the upper right panel of Fig. 2 as ones with bluer colours than the member galaxies of the present cluster.

PSZ1 G109.14-28.02: In addition to the rich galaxy cluster at $z = 0.457$, there are two galaxy groups at $z = 0.234$ (the redshift of one of these groups was also measured spectroscopically at RTT150), a nearby elliptical galaxy at $z = 0.0418$ (2MASX J23524477+3319474), and a bright star in the field (Fig. 15). The

Table 2. Clusters below the $4.5\,\sigma$ limit of the PSZ1 catalogue observed with the RTT150.

| Name | Position (J2000) | | | New ID |
	R. A.	Decl.	z	
PLCK G201.42−56.60	03 08 18.1	−16 26 01	...	+
PLCK G210.76+08.02	07 16 08.1	+05 34 01	0.296	+
PLCK G201.03+29.90	08 23 55.5	+22 43 51	0.668[a]	+
PLCK G244.13+26.11	09 24 06.2	−12 19 05	...	+
PLCK G164.28+52.61	10 16 19.9	+50 10 29	0.488	
PLCK G041.62+57.43	15 18 22.3	+27 10 18	...	+
PLCK G050.55−25.00	20 51 56.4	+02 56 43	...	+

[a] Measured at the BTA 6-m telescope of SAO RAS.
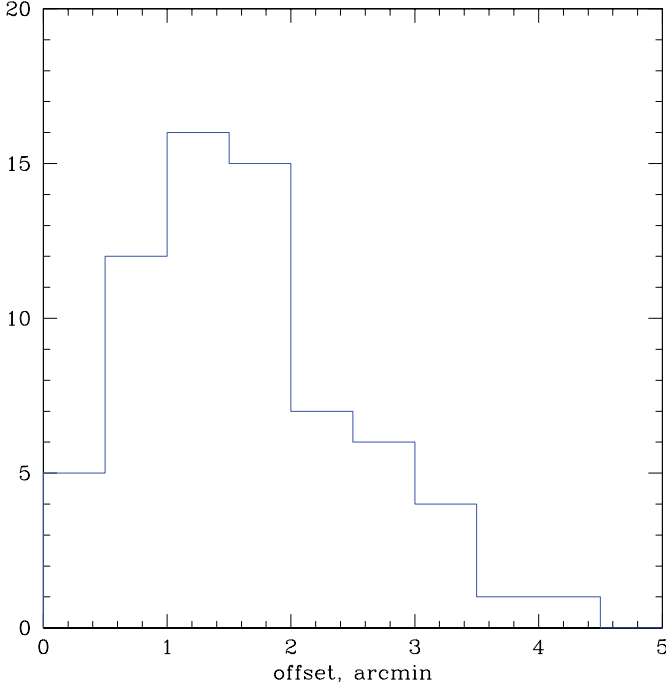
Fig. 6. The distribution of cluster optical centres offsets relative to their SZ position measured with *Planck*.

main part of the SZ signal detected by *Planck* is most probably produced by the rich cluster at $z = 0.457$; however, other objects may also affect the photometry of the detected SZ source.

PSZ1 G227.89+36.58: This cluster is at $z \approx 0.47$. There is also a foreground group offset by about $4'$ to the SW at $z = 0.2845$ (ZwCl 0924.4+0511, MaxBCG J141.76983+04.97937). From comparison of optical richnesses, we conclude that the cluster at $z \approx 0.47$ is much more massive, and should produce most of the SZ signal detected by *Planck*. The SZ photometry, however, may be affected by the foreground group.

6.3. Complicated cases

In a few cases, optical data are not sufficient to reliably identify observed SZ sources. In order to determine the nature of these objects, additional SZ or X-ray data are needed.

PSZ1 G103.50+31.36: This SZ source may be identified with an irregular group of galaxies (Fig. 16). Its redshift can be estimated photometrically as $z \approx 0.238$; however, the very bright star HR 6606 ($m_V = 5.8$) is located at the edge of the field, about $5\rlap{.}'6$ from the *Planck* position. HR 6606 is detected by *Planck* with flux density about 1 Jy at 857 GHz (Planck Collaboration XXVIII 2013), and probably affects the photometry of the detected SZ source, artificially increasing its significance.

PSZ1 G115.70+17.51: There is a group of galaxies with red sequence colour corresponding to a redshift of $z \approx 0.50$ near the centroid of the SZ detection (Fig. 17), and also a few galaxies at $z = 0.1112$ (measured spectroscopically at RTT). Hovever, there is a lot of Galactic cirrus in the field, as well as a very bright star (HR 8550, $m_V = 6.8$) approximately $7'$ from the SZ position, which is detected by *Planck* at 857 GHz (where the expected SZ increment is negligible) at about 10 Jy (Planck Collaboration XXVIII 2013). Both the cirrus and the star likely affect the SZ signal detected by *Planck*.

We obtained deep r' and i' images with the RTT150 for nine more objects from the PSZ1 cluster catalogue (G037.67+15.71, G115.34-54.89, G115.59-44.47, G146.00-49.42, G159.26+71.11, G167.43-38.04, G184.50-55.73, G194.68-49.73, and G199.70+37.01) and for 30 sources from intermediate versions of the *Planck* catalogue that were eventually not confirmed as part of the PSZ1 catalogue. Out of the nine sources from the PSZ1 catalogue, in four cases (G037.67+15.71, G159.26+71.11, G184.50-55.73, and G199.70+37.01) we detected a few elliptical galaxies in the field, which, however, cannot be identified as a galaxy cluster on the basis of our data. In the other cases, bright stars (G115.34-54.89 and G146.00-49.42) and Galactic cirrus (G115.59-44.47, G167.43-38.04, and G146.00-49.42) most probably affect the measurements. We conservatively maintained these objects in the PSZ1 catalogue; however, they will need to be assessed in the future by additional observations, in particular in X-rays.

7. Conclusions

This article is a companion paper to the *Planck* catalogue of SZ sources published in Planck Collaboration XXIX (2013). We present here the results of approximately three years of optical observations of *Planck* SZ sources with the Russian-Turkish 1.5-m telescope. Approximately 60 clear dark and grey nights — 20 % of the total clear dark and grey time at the telescope during that period — were used for these observations. We also used approximately 32 hours of clear weather at the BTA 6-m telescope of the SAO RAS.
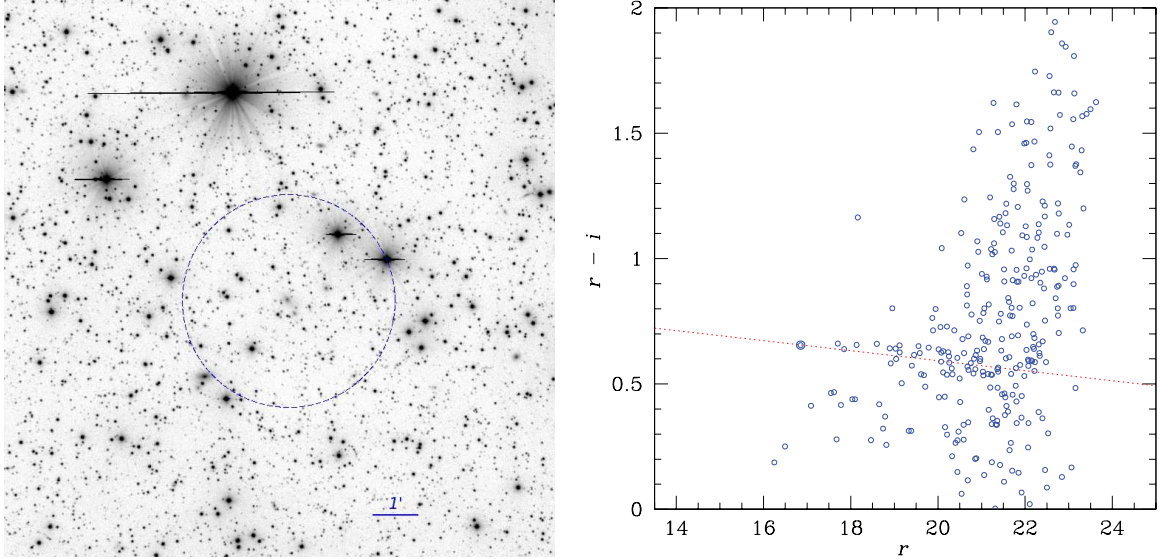
Fig. 7. PSZ1 G060.12+11.42, a cluster at low Galactic latitude ($b \approx -11°4$). *Left*: i'-band RTT150 image. *Right*: colour-magnitude diagram of extended objects near the cluster centre in the area enclosed by the dashed circle in the left panel. The dotted line indicates the red sequence.
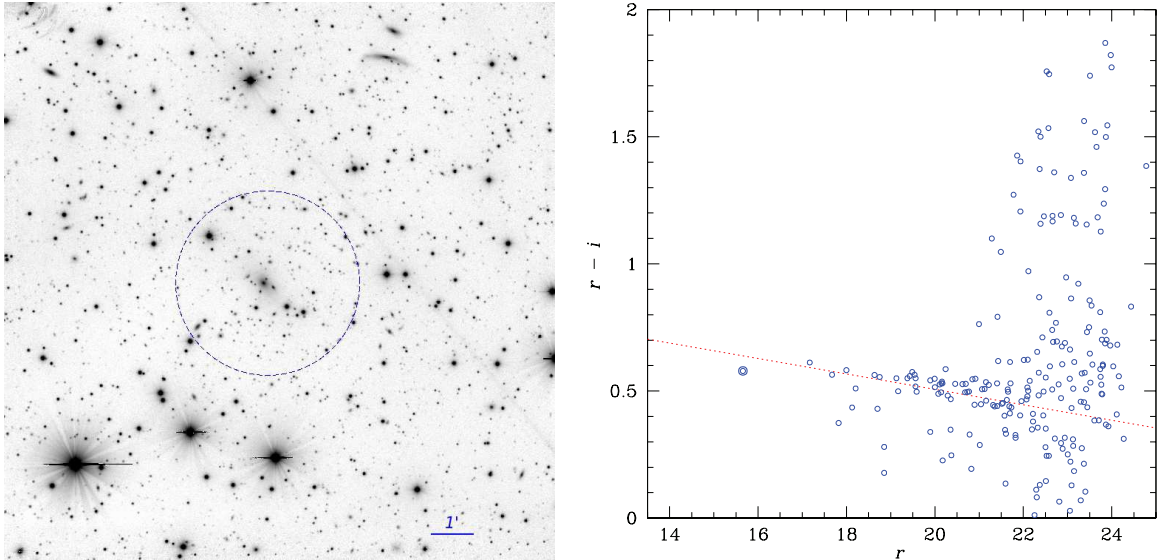

Fig. 8. PSZ1 G076.44+23.53, a cluster that could be classified as a fossil group (e.g., Voevodkin et al. 2010). *Left*: i'-band RTT150 image. *Right*: colour-magnitude diagram of extended objects near the cluster centre in the area enclosed by the dashed circle in the left panel. The dotted line indicates the red sequence.

In total, deep direct images were obtained of more than one hundred fields in multiple filters. We identified 47 previously unknown clusters, 41 of which were included in the PSZ1 catalogue, and selected galaxies to be used in determining cluster redshifts. We measured redshifts of 65 *Planck* clusters, including the redshifts of 12 distant clusters measured at the 6-m BTA telescope. Thirty-one of these redshifts were measured after publication of the PSZ1 catalogue (Planck Collaboration XXIX 2013) and are published here for the first time. For 14 more clusters, we give photometric redshift estimates. Some clusters with only

a few elliptical galaxies or with possible contamination by stars and galactic dust have been kept in the PSZ1 catalogue.

We identified six cases of projections (see Sect. 6.2) among the clusters identified in our work. A similar result was obtained earlier with a sample of *Planck* clusters validated using *XMM-Newton* X-ray observations (Planck Collaboration Int. IV 2013). The fraction of projected clusters seems to be higher than in other surveys. For example, only six out of about 200 clusters, either in the *400d* X-ray galaxy cluster survey (Burenin et al.
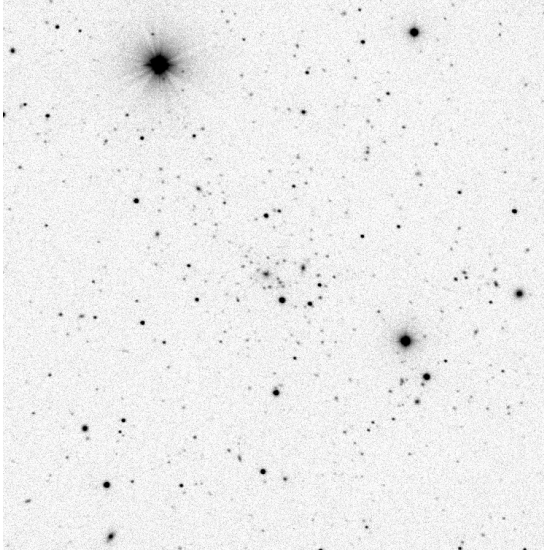
Fig. 9. PSZ1 G048.22-65.03   RTT150 *r′*-band image. This cluster is too distant to be identified with DSS ($z \approx 0.42$) and there are no SDSS data in this field.
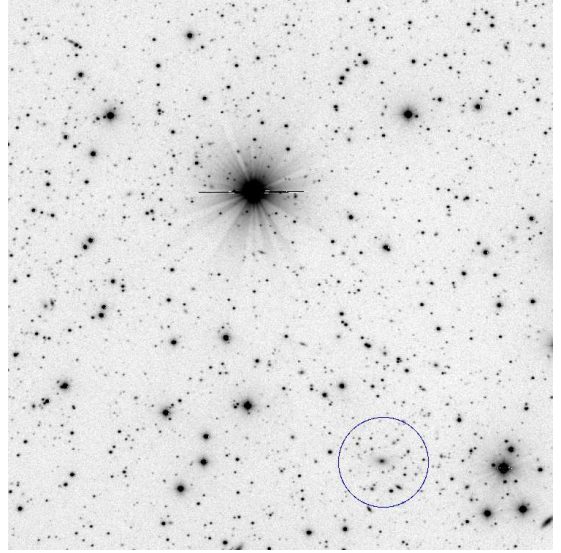
Fig. 11. PSZ1 G066.01-23.30   RTT150 *i′*-band image centred on the *Planck* SZ source coordinates. The position of the optical galaxy cluster is shown with a circle.
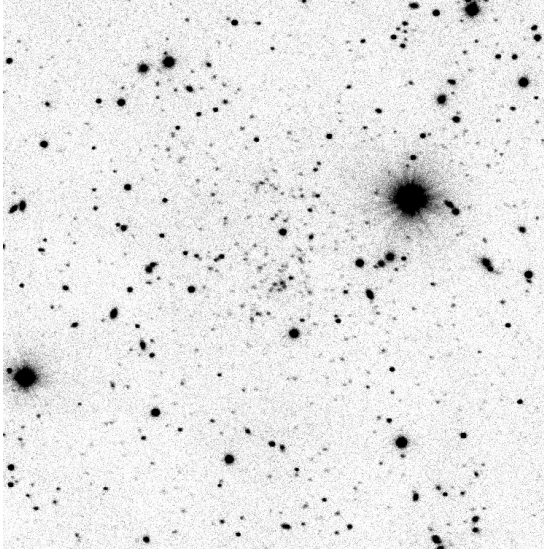

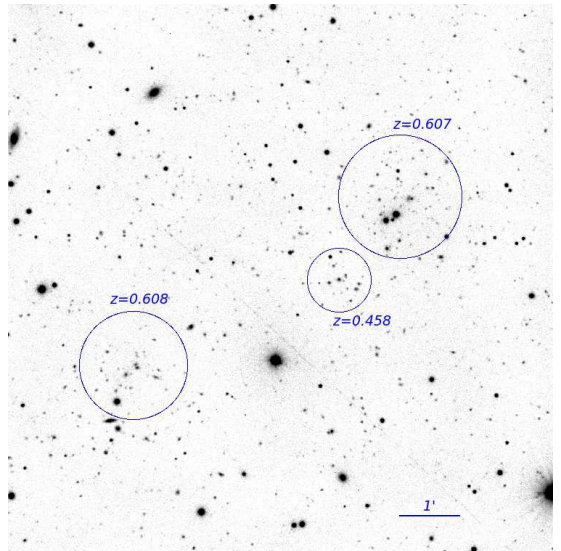**Fig. 10.** PSZ1 G084.04+58.75   RTT150 *i′*-band image. This cluster is too distant to be identified with SDSS ($z = 0.731$).

Fig. 12. PSZ1 G070.91+49.26   RTT150 *i′*-band image centred on the *Planck* SZ source coordinates. In addition to a double cluster at $z \approx 0.61$, there is a smaller foreground cluster at $z \approx 0.46$.

2007) or in the South Pole Telescope SZ survey (Reichardt et al. 2012), are detected at $< 10′$ angular separation.

We emphasize that the sub-sample of *Planck* SZ sources studied in our work is not statistically representative in any sense. The sources observed at the RTT150 were selected from different versions of the *Planck* SZ source catalogue during a two-year period. It is therefore impossible to quantify biases in the selection of sources from the *Planck* catalogue for follow-up in this programme. If a high fraction of projections is determined in a statistically representative sample of *Planck* clusters, it would imply that the detection probability of projected clusters is significantly enhanced in the *Planck* data, and that projection effects should be taken into account in statistical calibration of the *Planck* catalogue.

In particular, it is not possible to estimate a fraction of false sources in the *Planck* SZ survey from the RTT150 sample only.

We might expect this fraction to be larger in the RTT150 sample than in the full PSZ1 sample, since a large number of "good" clusters immediately identified in the PSZ1 sample using DSS and SDSS data were excluded from the RTT150 sample. But, on the other hand, targets for observations were selected to confirm candidates suspected of being clusters on the basis of other optical and IR data.

The RTT150 images typically reach $m_{i′} = 23$ mag. Our study shows that imaging data from a 1.5-m class telescope can be used successfully to identify clusters below the SDSS limit ($z \approx 0.6$) at redshifts up to $z \approx 1$, and also in fields where no SDSS imaging data exist, e.g., at low Galactic latitudes in the North. A negative result in our optical identification programme does not necessarily mean that an SZ detection is false. Yet more distant
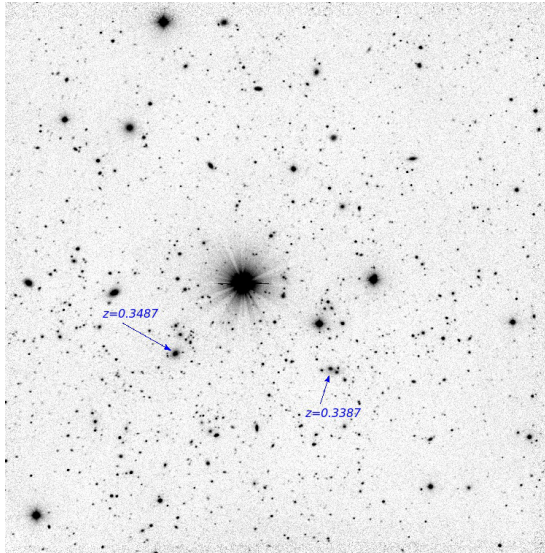
Fig. 13. PSZ1 G092.27-55.73 RTT150 i'-band image. Two cD galaxies and their redshifts are shown.
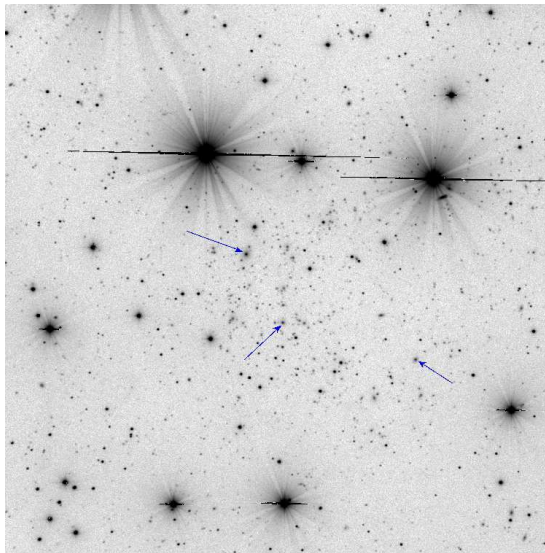

Fig. 14. PSZ1 G100.18-29.68 RTT150 i'-band image. The arrows indicate foreground elliptical galaxies.
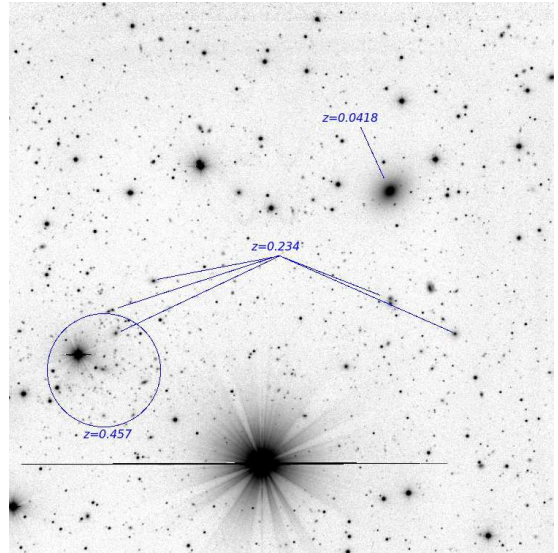

Fig. 15. PSZ1 G109.14-28.02 RTT150 i'-band image. In addition to the rich cluster at $z = 0.457$, there are also two galaxy groups at $z = 0.234$, a nearby elliptical galaxy at $z = 0.0418$, and a bright star in the field.
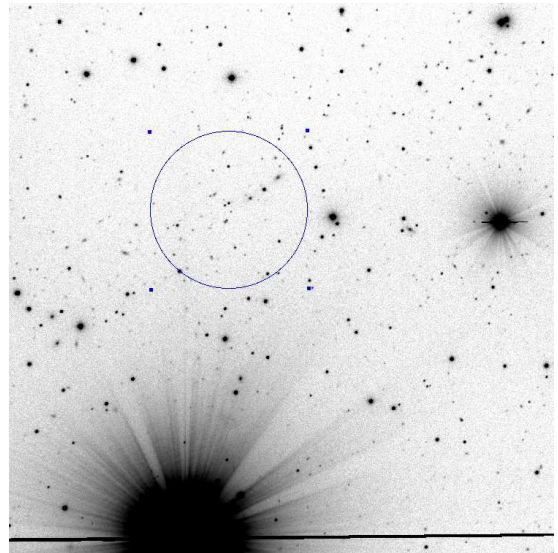

Fig. 16. PSZ1 G103.50+31.36 RTT150 i'-band image centred on the coordinates of the SZ source detected by *Planck*, identified with the galaxy group shown in the circle. However, there is also a very bright star ($m_V = 5.8$) at the edge of the field, $5'.6$ from the *Planck* position and detected by *Planck*, which most probably affects the SZ signal.

clusters may be identified using better optical data and also with better data in the SZ and X-ray domains. Follow-up programmes are now also running at other telescopes — NOT, INT, GTC, TNG, WHT, NTT, and others — and optical identifications of *Planck* cluster candidates could be completed within a few years.

References

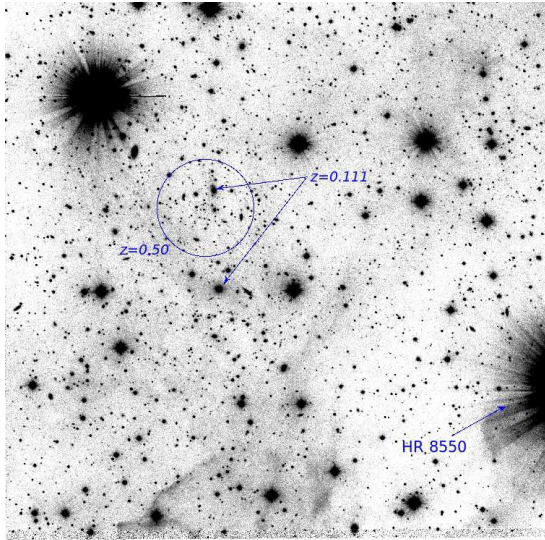Aihara, H., Allende Prieto, C., An, D., et al. 2011, ApJS, 193, 29

Fig. 17. PSZ1 G115.70+17.51   RTT150 i'-band image, centred on the coordinates of the SZ source detected by *Planck*, which may be identified with the galaxy group shown in the circle. However, there are Galactic cirrus clouds throughout the field, and a very bright star ($m_V = 6.8$) about 7′ away, which most probably affect the SZ signal.

Aslan, Z., Bikmaev, I. F., Vitrichenko, É. A., et al. 2001, Astronomy Letters, 27, 398

Bertin, E., & Arnouts, S. 1996, A&AS, 117, 393

Burenin, R. A., Vikhlinin, A., Hornstrup, A., Ebeling, H., Quintana, H., Mescheryakov, A. 2007, ApJS, 172, 56

Gladders, M. D., Yee, H. K. C. AJ, 120, 2148

Jones, L. R., Ponman, T. J., Horton, A., et al. 2003, MNRAS, 343, 627

Moiseev A. V., Afanasyev V. L., 2005, Astronomy Letters, 31, 194

Mullis, C. R., McNamara, B. R., Quintana, H., Vikhlinin, A., Henry, J. P., Gioia, I. M., Hornstrup, A., Forman, W., Jones, C., 2003, ApJ, 594, 154

Planck Collaboration VIII. 2011, A&A, 536, A8

Planck Collaboration IX. 2011, A&A, 536, A9

Planck Collaboration. 2011, A&A, 536, A9

Planck Collaboration Int. I. 2012, A&A, 543, A102

Planck Collaboration Int. IV. 2013, A&A, 550, A130

Planck, AMI Collaborations. 2013, A&A, 550, A128

Planck Collaboration. 2012, A&A, in press; arXiv:1205.3376

Planck Collaboration XXIX: Ade, P. A. R., Aghanim, N., Armitage-Caplan, C., et al. 2013, A&A, in press; arXiv:1303.5089

Planck Collaboration XXVIII: Ade, P. A. R., Aghanim, N., Argüeso, et al. 2013, A&A, in press; arXiv:1303.5088

Ponman, T. J., Allan, D. J., Jones, L. R., et al. 1994, Nature, 369, 462

Sunyaev, R. A., Zeldovich, Y. B. 1972, Comments on Astrophysics and Space Physics, 4, 173

Reichardt, C. L., Stalder B., Bleem L. E., et al., 2013, ApJ, 763, 127

Vikhlinin, A., McNamara, B. R., Hornstrup, A., et al. 1999, ApJ, 520, L1

Vikhlinin, A., McNamara, B. R., Forman, W., et al. 1998 ApJ, 502, 558

Vikhlinin, A., Burenin, R. A., Ebeling, H., et al. 2009, ApJ, 692, 1033

Veilleux, S., Osterbrock, D. E. 1987, ApJS, 63, 295

Voevodkin, A., Borozdin, K., Heitmann, K., et al. 2010, ApJ, 708, 1376

Voges, W., Aschenbach, B., Boller, Th., et al. 1999, A&A, 349, 389

Voges, W., Aschenbach, B., Boller, Th., et al. 2000, IAU Circ., 7432, 3

Wright, E. L., Eisenhardt, P. R. M., Mainzer, A. K., et al. 2010, AJ, 140, 1868

Wen, Z. L., Han, J. L., Liu, F. S., ApJS, 2012, 199, 34

[1] APC, AstroParticule et Cosmologie, Université Paris Diderot, CNRS/IN2P3, CEA/lrfu, Observatoire de Paris, Sorbonne Paris Cité, 10, rue Alice Domon et Léonie Duquet, 75205 Paris Cedex 13, France

[2] Academy of Sciences of Tatarstan, Bauman Str., 20, Kazan, 420111, Republic of Tatarstan, Russia

[3] African Institute for Mathematical Sciences, 6-8 Melrose Road, Muizenberg, Cape Town, South Africa

[4] Agenzia Spaziale Italiana Science Data Center, Via del Politecnico snc, 00133, Roma, Italy

[5] Agenzia Spaziale Italiana, Viale Liegi 26, Roma, Italy

[6] Astrophysics Group, Cavendish Laboratory, University of Cambridge, J J Thomson Avenue, Cambridge CB3 0HE, U.K.

[7] Astrophysics & Cosmology Research Unit, School of Mathematics, Statistics & Computer Science, University of KwaZulu-Natal, Westville Campus, Private Bag X54001, Durban 4000, South Africa

[8] Atacama Large Millimeter/submillimeter Array, ALMA Santiago Central Offices, Alonso de Cordova 3107, Vitacura, Casilla 763 0355, Santiago, Chile

[9] CITA, University of Toronto, 60 St. George St., Toronto, ON M5S 3H8, Canada

[10] CNRS, IRAP, 9 Av. colonel Roche, BP 44346, F-31028 Toulouse cedex 4, France

[11] California Institute of Technology, Pasadena, California, U.S.A.

[12] Centro de Estudios de Física del Cosmos de Aragón (CEFCA), Plaza San Juan, 1, planta 2, E-44001, Teruel, Spain

[13] Computational Cosmology Center, Lawrence Berkeley National Laboratory, Berkeley, California, U.S.A.

[14] DSM/Irfu/SPP, CEA-Saclay, F-91191 Gif-sur-Yvette Cedex, France

[15] DTU Space, National Space Institute, Technical University of Denmark, Elektrovej 327, DK-2800 Kgs. Lyngby, Denmark

[16] Département de Physique Théorique, Université de Genève, 24, Quai E. Ansermet,1211 Genève 4, Switzerland

[17] Departamento de Física, Universidad de Oviedo, Avda. Calvo Sotelo s/n, Oviedo, Spain

[18] Department of Astronomy and Geodesy, Kazan Federal University, Kremlevskaya Str., 18, Kazan, 420008, Russia

[19] Department of Astrophysics/IMAPP, Radboud University Nijmegen, P.O. Box 9010, 6500 GL Nijmegen, The Netherlands

[20] Department of Physics & Astronomy, University of British Columbia, 6224 Agricultural Road, Vancouver, British Columbia, Canada

[21] Department of Physics and Astronomy, Dana and David Dornsife College of Letter, Arts and Sciences, University of Southern

California, Los Angeles, CA 90089, U.S.A.

[22] Department of Physics and Astronomy, University College London, London WC1E 6BT, U.K.

[23] Department of Physics, Florida State University, Keen Physics Building, 77 Chieftan Way, Tallahassee, Florida, U.S.A.

[24] Department of Physics, Gustaf Hällströmin katu 2a, University of Helsinki, Helsinki, Finland

[25] Department of Physics, Princeton University, Princeton, New Jersey, U.S.A.

[26] Department of Physics, University of California, Santa Barbara, California, U.S.A.

[27] Department of Physics, University of Illinois at Urbana-Champaign, 1110 West Green Street, Urbana, Illinois, U.S.A.

[28] Dipartimento di Fisica e Astronomia G. Galilei, Università degli Studi di Padova, via Marzolo 8, 35131 Padova, Italy

[29] Dipartimento di Fisica e Scienze della Terra, Università di Ferrara, Via Saragat 1, 44122 Ferrara, Italy

[30] Dipartimento di Fisica, Università La Sapienza, P. le A. Moro 2, Roma, Italy

[31] Dipartimento di Fisica, Università degli Studi di Milano, Via Celoria, 16, Milano, Italy

[32] Dipartimento di Fisica, Università di Roma Tor Vergata, Via della Ricerca Scientifica, 1, Roma, Italy

[33] Discovery Center, Niels Bohr Institute, Blegdamsvej 17, Copenhagen, Denmark

[34] Dpto. Astrofísica, Universidad de La Laguna (ULL), E-38206 La Laguna, Tenerife, Spain

[35] European Southern Observatory, ESO Vitacura, Alonso de Cordova 3107, Vitacura, Casilla 19001, Santiago, Chile

[36] European Space Agency, ESAC, Planck Science Office, Camino bajo del Castillo, s/n, Urbanización Villafranca del Castillo, Villanueva de la Cañada, Madrid, Spain

[37] European Space Agency, ESTEC, Keplerlaan 1, 2201 AZ Noordwijk, The Netherlands

[38] Facoltà di Ingegneria, Università degli Studi e-Campus, Via Isimbardi 10, Novedrate (CO), 22060, Italy

[39] HGSFP and University of Heidelberg, Theoretical Physics Department, Philosophenweg 16, 69120, Heidelberg, Germany

[40] Helsinki Institute of Physics, Gustaf Hällströmin katu 2, University of Helsinki, Helsinki, Finland

[41] INAF - Osservatorio Astronomico di Padova, Vicolo dell'Osservatorio 5, Padova, Italy

[42] INAF - Osservatorio Astronomico di Roma, via di Frascati 33, Monte Porzio Catone, Italy

[43] INAF - Osservatorio Astronomico di Trieste, Via G.B. Tiepolo 11, Trieste, Italy

[44] INAF/IASF Bologna, Via Gobetti 101, Bologna, Italy

[45] INAF/IASF Milano, Via E. Bassini 15, Milano, Italy

[46] INFN, Sezione di Bologna, Via Irnerio 46, I-40126, Bologna, Italy

[47] INFN, Sezione di Roma 1, Università di Roma Sapienza, Piazzale Aldo Moro 2, 00185, Roma, Italy

[48] Imperial College London, Astrophysics group, Blackett Laboratory, Prince Consort Road, London, SW7 2AZ, U.K.

[49] Infrared Processing and Analysis Center, California Institute of Technology, Pasadena, CA 91125, U.S.A.

[50] Institut Universitaire de France, 103, bd Saint-Michel, 75005, Paris, France

[51] Institut d'Astrophysique Spatiale, CNRS (UMR8617) Université Paris-Sud 11, Bâtiment 121, Orsay, France

[52] Institut d'Astrophysique de Paris, CNRS (UMR7095), 98 bis Boulevard Arago, F-75014, Paris, France

[53] Institute for Space Sciences, Bucharest-Magurale, Romania

[54] Institute of Astronomy, University of Cambridge, Madingley Road, Cambridge CB3 0HA, U.K.

[55] Institute of Theoretical Astrophysics, University of Oslo, Blindern, Oslo, Norway

[56] Instituto de Astrofísica de Canarias, C/Vía Láctea s/n, La Laguna, Tenerife, Spain

[57] Instituto de Física de Cantabria (CSIC-Universidad de Cantabria), Avda. de los Castros s/n, Santander, Spain

[58] Jet Propulsion Laboratory, California Institute of Technology, 4800 Oak Grove Drive, Pasadena, California, U.S.A.

[59] Jodrell Bank Centre for Astrophysics, Alan Turing Building, School of Physics and Astronomy, The University of Manchester, Oxford

Road, Manchester, M13 9PL, U.K.

[60] Kavli Institute for Cosmology Cambridge, Madingley Road, Cambridge, CB3 0HA, U.K.

[61] LAL, Université Paris-Sud, CNRS/IN2P3, Orsay, France

[62] LERMA, CNRS, Observatoire de Paris, 61 Avenue de l'Observatoire, Paris, France

[63] Laboratoire AIM, IRFU/Service d'Astrophysique - CEA/DSM - CNRS - Université Paris Diderot, Bât. 709, CEA-Saclay, F-91191 Gif-sur-Yvette Cedex, France

[64] Laboratoire de Physique Subatomique et de Cosmologie, Université Joseph Fourier Grenoble I, CNRS/IN2P3, Institut National Polytechnique de Grenoble, 53 rue des Martyrs, 38026 Grenoble cedex, France

[65] Laboratoire de Physique Théorique, Université Paris-Sud 11 & CNRS, Bâtiment 210, 91405 Orsay, France

[66] Lawrence Berkeley National Laboratory, Berkeley, California, U.S.A.

[67] Max-Planck-Institut für Astrophysik, Karl-Schwarzschild-Str. 1, 85741 Garching, Germany

[68] Max-Planck-Institut für Extraterrestrische Physik, Giessenbachstraße, 85748 Garching, Germany

[69] McGill Physics, Ernest Rutherford Physics Building, McGill University, 3600 rue University, Montréal, QC, H3A 2T8, Canada

[70] Moscow Institute of Physics and Technology, Dolgoprudny, Institutsky per., 9, 141700, Russia

[71] National University of Ireland, Department of Experimental Physics, Maynooth, Co. Kildare, Ireland

[72] Niels Bohr Institute, Blegdamsvej 17, Copenhagen, Denmark

[73] SISSA, Astrophysics Sector, via Bonomea 265, 34136, Trieste, Italy

[74] School of Physics and Astronomy, Cardiff University, Queens Buildings, The Parade, Cardiff, CF24 3AA, U.K.

[75] Space Research Institute (IKI), Russian Academy of Sciences, Profsoyuznaya Str, 84/32, Moscow, 117997, Russia

[76] Space Sciences Laboratory, University of California, Berkeley, California, U.S.A.

[77] Special Astrophysical Observatory, Russian Academy of Sciences, Nizhnij Arkhyz, Zelenchukskiy region, Karachai-Cherkessian Republic, 369167, Russia

[78] Sub-Department of Astrophysics, University of Oxford, Keble Road, Oxford OX1 3RH, U.K.

[79] TÜBİTAK National Observatory, Akdeniz University Campus, 07058, Antalya, Turkey

[80] UPMC Univ Paris 06, UMR7095, 98 bis Boulevard Arago, F-75014, Paris, France

[81] Université de Toulouse, UPS-OMP, IRAP, F-31028 Toulouse cedex 4, France

[82] University of Granada, Departamento de Física Teórica y del Cosmos, Facultad de Ciencias, Granada, Spain

[83] University of Granada, Instituto Carlos I de Física Teórica y Computacional, Granada, Spain

[84] Warsaw University Observatory, Aleje Ujazdowskie 4, 00-478 Warszawa, Poland